YALE JOURNAL OF BIOLOGY AND MEDICINE 66 (1993), pp. 157–163

A Defect-in-Continuity in the Canine Femur: and *In-Vivo* Experimental Model for the Study of Bone Graft Incorporation

Ronald W. Lindsey, M.D.[a], Theodore Miclau, M.D.[b], Robert Probe, M.D.[c], and Stephan Perren, M.D.[d]

[a]*Department of Orthopaedic Surgery, Baylor College of Medicine, Houston, Texas*

[b]*Department of Orthopaedics, University of North Carolina, Chapel Hill, North Carolina*

[c]*Department of Orthoapedics, Scott & White Clinic, Temple, Texas*

[d]*Laboratorium Für experimentelle Chirurgie, Schweizerisches Forschüngsinstitut, Switzerland*

(Submitted March 8, 1993; sent for revision April 3; received and accepted May 20, 1993)

The *in-vivo* study of bone graft incorporation has traditionally used a segmental diaphyseal bone defect. This model reliably produces a nonunion, but is complicated by graft instability and altered limb loading stresses. The authors discuss the advantages of a defect-in-continuity canine femur model which produces a more consistent union with fewer mechanical complications despite the absence of fixation. This proposed model permits analysis of radiographic, histologic and biomechanical data which are more applicable to the usual clinical setting in which bone graft is required.

INTRODUCTION

Bone graft is commonly employed to promote fracture healing [1]. Most studies examining bone graft incorporation have used a segmental defect model in diaphyseal bone. Although this model produces complete strength diminution, [2, 3] the segmental defect model is compromised by the need for supplementary fixation, potential graft displacement, and frequent nonunion [4, 5].

An experimental model utilizing a partial defect in otherwise intact bone (defect-in-continuity) protects graft material, is inherently stable, obviates the need for supplemental fixation, and is less apt to be complicated by nonunion [6]. In addition, a defect-in-continuity is more representative of the usual clinical situations requiring bone grafting than is the segmental defect.

The purpose of this study was to determine if a defect-in-continuity canine model for bone graft incorporation could be employed *in vivo* without supplemental fixation, avoid frequent limb fracture, yet provide an experimental model for radiographic, biomechanical, and histologic graft analysis.

MATERIALS AND METHODS

Twenty-nine fully immunized and quarantined adult mongrel dogs weighing 19–24 kilograms were obtained. Maturity was confirmed by x-ray examination of the distal femoral physes. Under sterile operating room conditions, a lateral surgical approach was

[a]*To whom correspondence should be addressed.* Ronald W. Lindsey, M.D., Department of Orthopaedic Surgery, 6550 Fannin, Suite 2625, Houston, Texas, 77030.

performed to the mid-diaphysis of both femurs. A standard oblong unicortical defect measuring 4.5mm x 30mm was created in the anterolateral femoral cortex using a trephine inserted under power into guide holes (Figure 1). The 4.5mm wide defect width reliably exceeded 20% of the bone's diameter which has been shown to decrease torsional strength 34 – 40% [7, 8] (mean outer diameter of 15.9 mm, mean inner diameter of 11.3 mm) (Figure 2). The oblong configuration with rounded edges minimizes the stress riser effect of the defect [9]. Pairs of cadaver femurs from adult dogs of comparable size were torsionally tested to failure to determine the strength of the defect versus intact bone.

The study was designed to be part of a broader experiment to examine the healing potential of a bone graft/antibiotic composite. Therefore, after the defect was curetted of all medullary tissue, 3 g of morselized autogenous bone graft was placed in one defect as the control, and 3 g of bone graft was mixed with 90 mg of tobramycin and placed in the contralateral defect. Autogenous bone graft was harvested from the proximal humerus, and the residual humeral defect was filled with methylmethacrylate. Fixation was not employed post-operatively. All animals were allowed to function immediately without restriction.

The animals were sacrificed at the following post-operative times: 1 week, 2 weeks, 3 weeks, 4 weeks, 6 weeks, and 12 weeks. All specimens were x-rayed with coronal and sagittal plain views post-operatively and at the time of sacrifice.

Following sacrifice at the respective time interval, the specimens were prepared for histological analysis. The femurs were cut at both ends to allow for penetration of the fixative into the marrow. The specimens were placed through a series of ascending alcohol solutions for 3 days each: 40%, 80%, 96%, 100%, and Xylol. The specimens were then placed in three different methylmethacrylate solutions for three days each (pure methylmethacrylate, 100 mL of methylmethacrylate plus 2 g of dibencoyl peroxide, and 100 mL of methylmethacrylate plus dibencoyl peroxide and 35 mL of plastoid). After fixation, the hardened methylmethacrylate bone was sectioned transversely into six blocks starting at 1 cm proximal to defect and continued at 1 cm intervals distally to 2 cm below the defect (Figure 3). From the proximal portion of each block, 3 200 mm sections were cut with a Leitz 1600 microtome. Two of the sections were ground between 75 – 90 micrometer thickness, and each stained with Giemsa and Fucsin, and mounted. The third 200 mm section was ground to a thickness between 40 – 60 micrometers and microradiographed with the Faxitron. The specimens were evaluated using a Zeiss light microscope.

Figure 1. The standard 4.5 mm x 30 mm oblong unicortical defect-in-continuity is demonstrated in the anterolateral mid-diaphysis cortex of a canine cadaver femur.

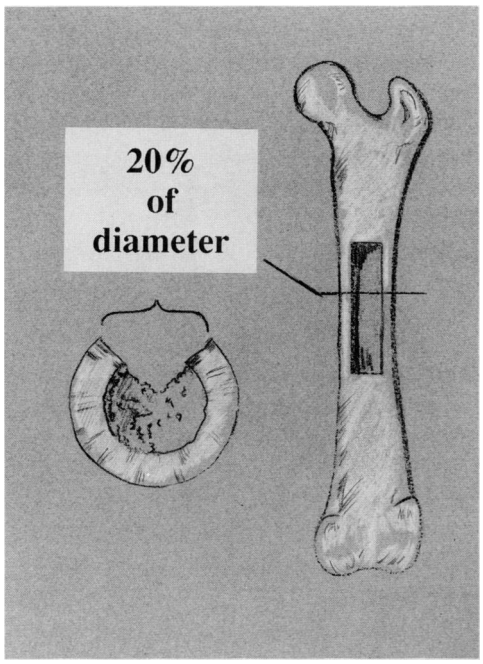

Figure 2. The defect's 4.5 mm width consistently exceeded 20% of the canine's femur mid-diaphysis diameter, thereby significantly decreasing the limb's torsional strength and permitting biomechanical assessment of graft healing.

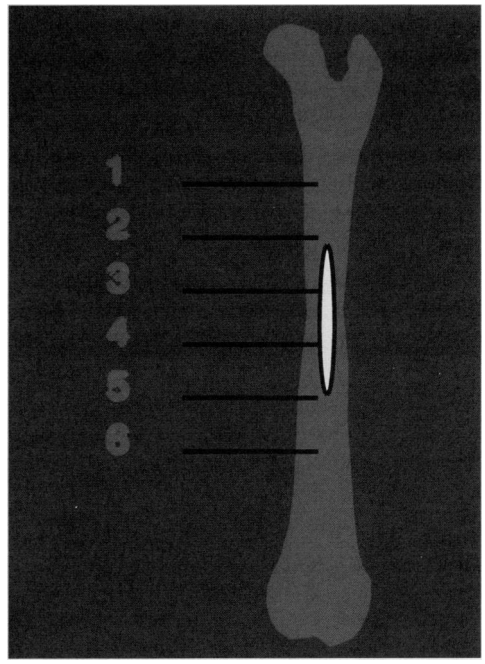

Figure 3. For histological analysis, transverse sections at varying intervals could be obtained both throughout the defect and at adjacent bone sites.

RESULTS

The paired cadaver specimens subjected to torsion testing demonstrated a mean torsional failure of the intact femur at 455 in/lb, and the defect-in-continuity limb at 195 in/lb. Therefore, the standard defect diminished strength by 42% of the intact strength. In twenty-nine dogs (fifty-eight limbs), seven fractures (12% of all limbs) occurred in six

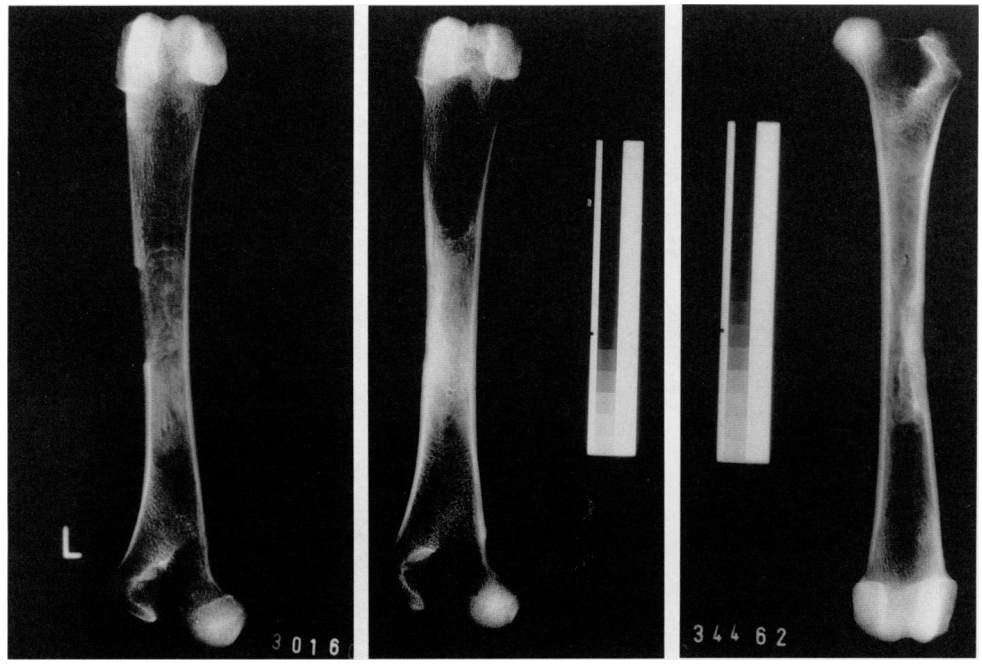

Figure 4 (A, B, and C). Radiographs of canine femurs sacrificed at 2, 6, and 12 weeks depict the progression of defect healing with reconstitution of the cortex and medullary canal.

dogs (20% of all dogs) prior to sacrifice. All fractures presented as a spiral fracture through the defect and occurred within the first two weeks at a mean of 6.2 days following surgery (range 2 – 14 days). There were no infections or cases of graft dislodgement.

Plain radiographs at 2, 6, and 12 weeks could easily quantitate the progression of healing of the defect (Figure 4). Detailed histologic and microradiographic analysis could be performed at varying levels of the defect permitting detailed study of not only graft incorporation at varying points in time, but also its effect on the adjacent intact bone (Figures 5, 6).

DISCUSSION

Segmental bone defects have historically provided an excellent *in-vivo* non-union model. When the defect is placed in the ulna or fibula of a limb with an intact radius or tibia, unrestricted activity can be maintained (weight-bearing) without the need for additional fixation [2, 5]. The defect creates complete strength diminution in the ulna/fibula, permitting excellent biomechanical monitoring of the healing bone graft. However, this model has been plagued by an extremely high complication rate which includes graft dislodgement, undesired nonunion, and infection report to be approximately 25% [2, 5]. Despite the presence of an intact radius or tibia, the normal loading stresses on the grafted ulna/fibula are altered in this model. Moreover, this type of defect does not represent the most common clinical setting requiring a bone graft.

Similar to same segmental defect models, the proposed defect-in-continuity model in

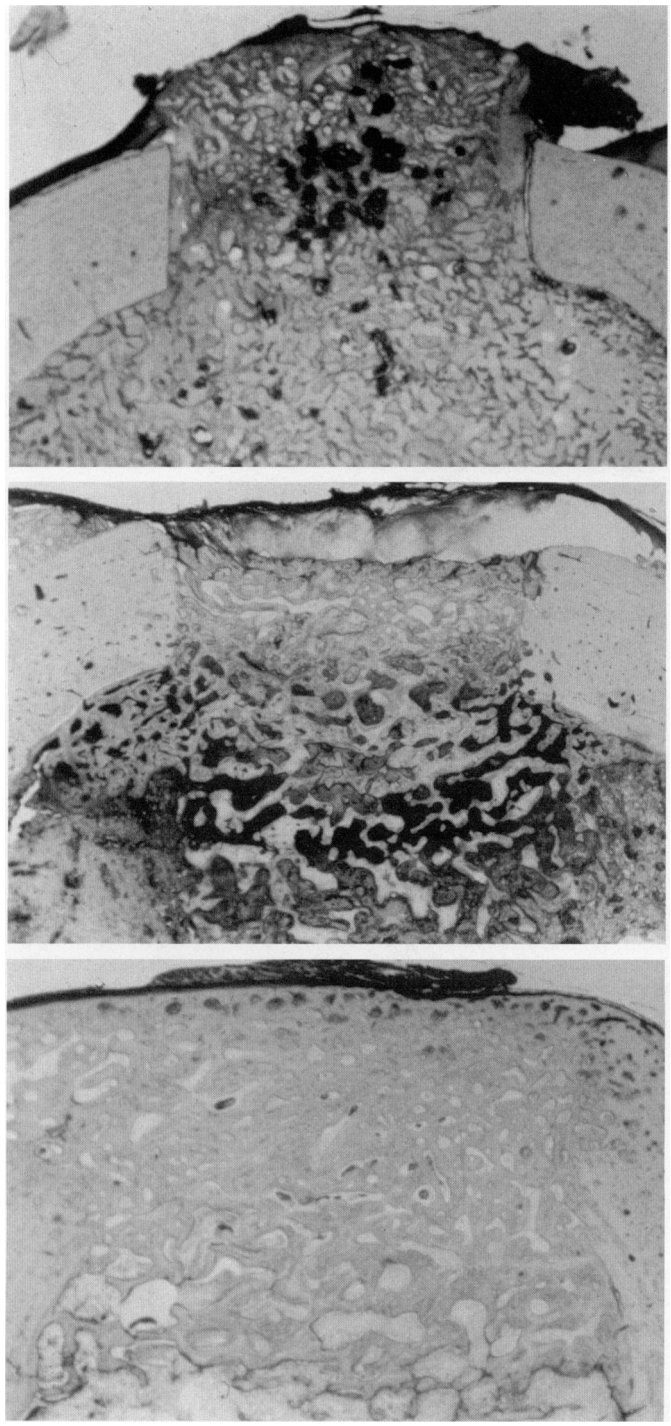

Figure 5 (A, B, and C). Histology sections through the defect at 2, 6, and 12 weeks permits temporal analysis of bone graft incorporation from a fibrous clot with sparse callus, to appositional bone formation on the graft's trabecular surface, to complete bridging of the defect by cortical compact bone.

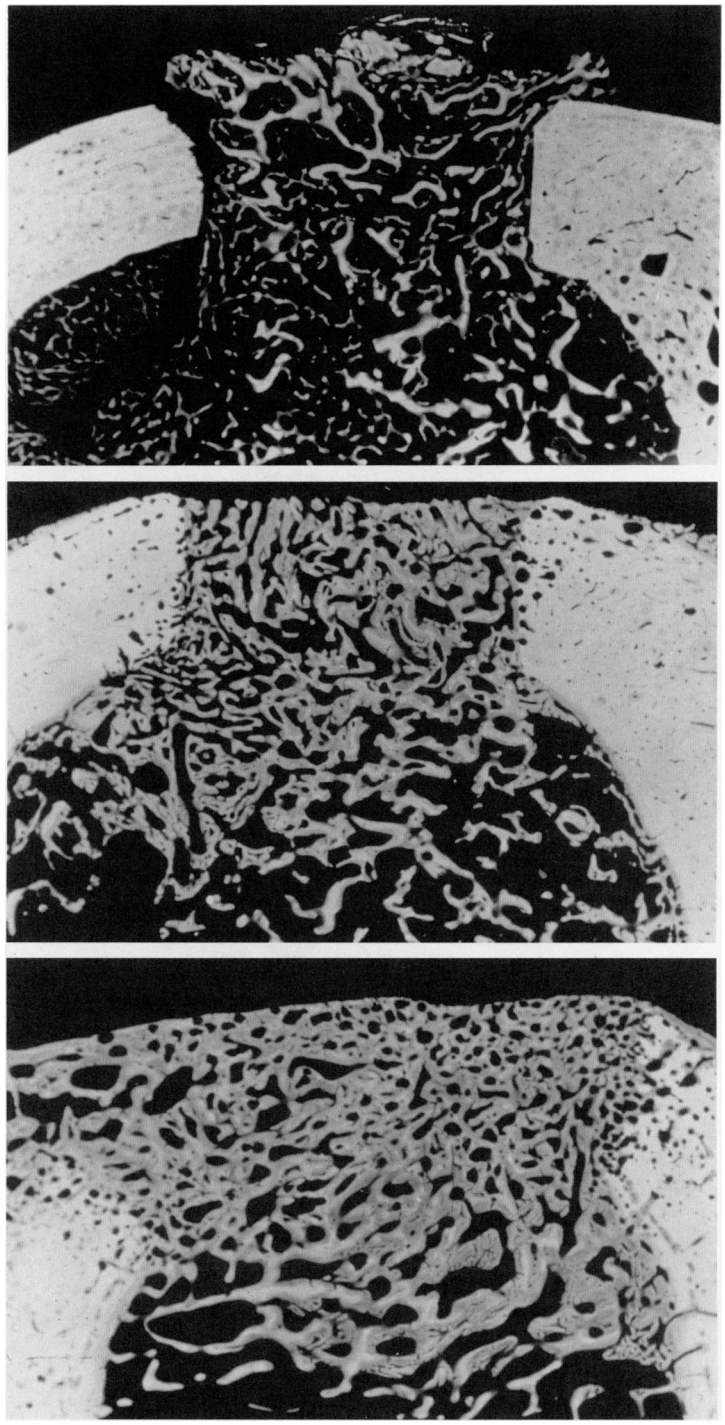

Figure 6 (A, B, and C). Micro-radiographs depict variations of the bone mineral density both within the graft material and at the adjacent intact cortical bone during the healing process at the same time intervals.

the canine femur does not require internal or external fixation. However, unlike the segmental defect model, the normal weight-bearing stresses in the grafted bone are not modified. Recently, Meadows et al. demonstrated that these cyclic loads enhanced the formation of bone in healing defects [10]. Therefore, in addition to protection from graft dislodgement, nonunion can be minimized. In the present series, the complication rate was favorable to that previously reported using segmental defects without altering the normal loading stresses.

The defect-in-continuity model permits the radiographic, microradiographic, and histologic assessment of graft incorporation. The proposed model can also depict the temporal progression of graft/intact bone interface healing at varying levels within the defect. The defect-in-continuity significantly reduces the torsional strength compared to the intact femur, allowing for biomechanical testing of the healing defect.

Therefore, the authors conclude that the defect-in-continuity canine model allows for an indepth analysis of bone graft incorporation *in vivo* with a minimum of adverse variables. In addition, the model better represents the more common clinical situation of a limb in partial continuity which requires supplemental grafting.

REFERENCES

1. Goldberg, V. M. and Stevenson, S. Natural history of autografts and allografts. Clin. Orthop. Rel. Res. 225:7–16, 1987.
2. Heiple, K. C., Chase, S. W., and Herndon, C. H. A comparative study of the healing process following different types of bone transplantation. J. Bone and Joint Surg. 45-A:1593–1612, 1963.
3. Einhorn, T. A., Lane, J. M., Burstein, A. H., Kopman, C. R., and Vigorita, V. J. The healing of segmental bone defects induced by demineralized bone matrix. J. Bone and Joint Surg. 66-A: 274–279, 1984.
4. Enneking, W. F., Burchardt, H., Puhl, J. J., and Piotrowski, G. Physical and biological aspects of repair in dog cortical-bone transplants. J. Bone and Joint Surg. 57-A:237–252, 1975.
5. Limeira dos Santos Neto, F. and Batista Volpon, J. Experimental nonunion in dogs. Clin. Orthop. Rel. Res. 187:260–271, 1984.
6. Shapiro, F. Cortical bone repair. J. Bone and Joint Surg. 70-A(7):1067–1081, 1988.
7. McBroom, R. J., Cheal, E. J., and Hayes, W. C. Strength reductions from metastatic cortical defects in long bones. Journal of Orthopaedic Res. 6:369–378, 1988.
8. Edgerton, B. C., An, K. N., and Morrey, B. F. Cortical Defects in Bone: An Analysis of the "Open-Section" *vs* "Stress Riser" effects under torsional load. Trans. 33rd ORS 12:191, 1987.
9. Clark, C. R., Morgan, C., Sonstegard, D. A., and Matthews, L. S. The effect of biopsy hole shape and size on bone strength. J. Bone and Joint Surg. 59-A:213–217, 1977.
10. Meadows, T. H., Bronk, J. T., Chao, E. Y. S., and Kelly, P. J. Effects of weight-bearing on healing of cortical defects in the canine tibia. J. Bone and Joint Surg. 72-A:1074–1080, 1990.